

Microscopic study of ^{240}Pu , mean-field and beyond

M. Bender and P.-H. Heenen

Service de Physique Nucléaire Théorique, Université Libre de Bruxelles, C.P. 229, B-1050 Bruxelles, Belgium

P. Bonche

Service de Physique Théorique CEA-Saclay, 91191 Gif sur Yvette Cedex, France

(Dated: August 12, 2004)

The influence of exact angular-momentum projection and configuration mixing on properties of a heavy, well-deformed nucleus is discussed for the example of ^{240}Pu . Starting from a self-consistent model using Skyrme interactions, we analyze the resulting modifications of the deformation energy, the fission barrier height, the excitation energy of the superdeformed minimum associated with the fission isomer, the structure of the lowest rotational bands with normal deformation and superdeformation, and the corresponding quadrupole moments and transition moments. We present results obtained with the Skyrme interactions SLy4 and SLy6, which have slightly different surface tensions.

PACS numbers: 21.60.Jz, 21.30.Fe, 21.10.-k, 27.90.+b

I. INTRODUCTION

Microscopic mean-field methods [1] are particularly well suited to describe nuclei with a well defined shape. When the energy of a nucleus depends softly on a shape degree of freedom or presents several minima as a function of this shape, correlations beyond mean field can affect the properties of the ground state strongly. In such cases, the two most relevant types of correlations are associated with the rotation of the nucleus and with its vibrations with respect to deformation. The inclusion of rotational correlations can be performed by a symmetry restoration and that of vibrations by a mixing of mean-field states corresponding to different shapes. In both cases, this requires to go beyond mean-field models.

We have recently developed a method which achieves these goals [2]. Applications have been carried out for neutron-deficient Pb isotopes [3, 4]. The low-energy spectrum of these nuclei varies rapidly with neutron number with states exhibiting strong mixing between oblate, spherical and prolate configurations. Qualitative properties of their spectra, including transition properties, were nicely explained. However, since the results depend strongly on the amount of mixing between several configurations, a detailed agreement with the data has not been achieved.

A very different situation occurs when the mean-field approximation is better justified as a first approximation, such as when coexisting states lie in well separated energy minima. This is the case at low excitation energies for superdeformed bands in nuclei around Hg and for fission isomers [5]. Nevertheless, it is only using beyond mean-field models that one can calculate spectra with well defined spin assignments as well as the corresponding transition probabilities.

The nucleus ^{240}Pu has often been used as a benchmark to study mean-field theories and effective interactions. We present here an application of our method to this nucleus. It will allow us to address the following issues:

(i) are quadrupole correlations influencing a well-

deformed nucleus *a priori* well-described by mean-field calculations?

(ii) how does the exact angular momentum projection modify the fission barrier and the excitation energy of fission isomers?

(iii) how much do the predictions depend upon different parameterizations of the effective interaction?

In what follows, we shortly recall the basic ingredients of the theory, then we present our results for the spectrum of ^{240}Pu in the ground state and the superdeformed well. The fission barrier obtained with two different effective interactions is discussed and compared with earlier, more phenomenological, approaches.

II. THE MODEL

The starting point of our method is a set of HF+BCS wave functions generated by self-consistent mean-field calculations with a constraint on a collective coordinate, the axial quadrupole moment $q = \langle Q_{20} \rangle$ in the present study. In the language of the spherical nuclear shell model, such mean-field states incorporate particle-particle (pairing) correlations as well as many-particle many-hole correlations by allowing deformations of the nucleus in its intrinsic frame. As a consequence, the mean-field states break several symmetries of the exact many-body states. This symmetry violation makes it difficult to relate mean-field results to spectroscopic data which are obtained in the laboratory frame of reference. The second step of our method is a restoration of the symmetries associated with particle numbers and rotation. Another ambiguity in the interpretation of mean-field results arises from the non-orthogonality of mean-field states corresponding to different quadrupole moments, so that different minima in a potential landscape cannot always be safely associated with different physical states. This difficulty is resolved in the third step of our method by variational mixing of symmetry-restored mean-field states corresponding to different quadrupole moments.

The method that we use is a discretized version of the generator coordinate method. It removes the contribution of vibrational excitations to the ground state and, at the same time, permits to construct a spectrum of excited states.

In our method, the same effective interaction is used to generate the mean-field states and to perform the configuration mixing. We present below results obtained with two different Skyrme interactions, SLy4 and SLy6 [6]. In both cases a density-dependent zero-range interaction is used in the pairing channel. We use the same strength as in previous studies, -1250 MeV fm 3 and two cutoffs, above and below the Fermi energy, as defined in Ref. [7]. The two Skyrme parameterizations differ mostly by their surface tension: the surface energy coefficient obtained from Hartree-Fock calculations of semi-infinite nuclear matter is lower for SLy6, 17.74 MeV, than for SLy4, 18.37 MeV [8]. Such a difference is expected to affect significantly the deformation energy at large quadrupole moments. Both parameterizations have been fitted in an identical way. Their differences have their origin in a different choice for the treatment of the spurious center-of-mass motion (c.m.): a fully variational c.m. one for SLy6 and a simpler one-body approximation for SLy4. The energy differences due to these two schemes induce slight differences in the properties of the interactions, see Ref. [9] for a detailed discussion.

As our main goal is an investigation of the overall effect of symmetry restoration and configuration mixing in a heavy, well-deformed nucleus, we restrict ourselves to axial and reflection-symmetric shape degrees of freedom. It has been shown that the fission barrier height obtained with SLy6 is in agreement with experiment within 1 MeV when octupole deformation is taken into account [1].

Our method has many interesting properties. Its sole phenomenological ingredient is the effective nucleon-nucleon interaction, which has been adjusted once and for all on generic nuclear properties. From a numerical point of view, it is simple enough to be applied throughout the mass table up to superheavy nuclei, utilizing the full model space of single-particle states with the proper coupling to the continuum. Another attractive aspect of the method is that it allows to determine electric transition probabilities directly in the laboratory frame between any pair of states. Finally, the method has the advantage that its results can be interpreted within the intuitive picture of intrinsic shapes and shells of single-particle states that is offered by the framework of mean-field models. More details on the method can be found in Refs. [2, 4].

Spectroscopic quadrupole moments and $B(E_\lambda)$ values are determined directly in the laboratory frame of reference [10]. To connect our results with other approaches, it is interesting to derive quantities analogous to intrinsic frame parameters from spectroscopic or transition moments. An intrinsic charge quadrupole moment $Q_{c2}^{(t)}(J, k)$

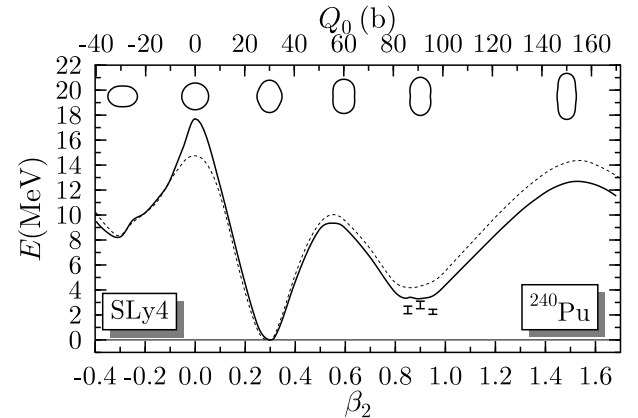


FIG. 1: Deformation energy curve of ^{240}Pu obtained with SLy4 projected on N and Z (dashed line) and projected on N , Z and $J = 0$ (solid line). All energies are normalized to the deformed ground-state value of each curve. The available experimental data for the excitation energy of the superdeformed band head are shown at arbitrary deformation (see text). Shapes along the path are indicated by the density contours at $\rho = 0.07$ fm $^{-3}$.

can be determined from $B(E_2)$ values:

$$Q_{c2}^{(t)}(J, k) = \sqrt{\frac{16\pi}{5} \frac{B(E2, J \rightarrow J-2)}{\langle J020|J-20\rangle^2 e^2}}, \quad (1)$$

or can be related to the spectroscopic quadrupole moment $Q_c(J, k)$ via the relation

$$Q_{c2}^{(s)}(J, k) = -\frac{2J+3}{J} Q_c(J, k). \quad (2)$$

We also adopt the sharp edge liquid drop relation to relate the β_2 deformation parameter and the axial quadrupole moment Q_2

$$\beta_2 = \sqrt{\frac{5}{16\pi}} \frac{4\pi Q_2}{3R^2 A} \quad , \quad (3)$$

where the nuclear radius R in fm at zero deformation is related to the mass A according to the standard formula $R = 1.2 A^{1/3}$.

III. RESULTS

A. Deformation energy

There is a large set of data on fission barriers of actinide nuclei [11, 12]. Among them, the double-humped fission barrier of ^{240}Pu has been used as a benchmark for mean-field models and effective interactions. First calculations were performed with Skyrme forces and the Hartree-Fock+BCS method [13], with the Gogny force and the HFB method [14] or with relativistic Lagrangians

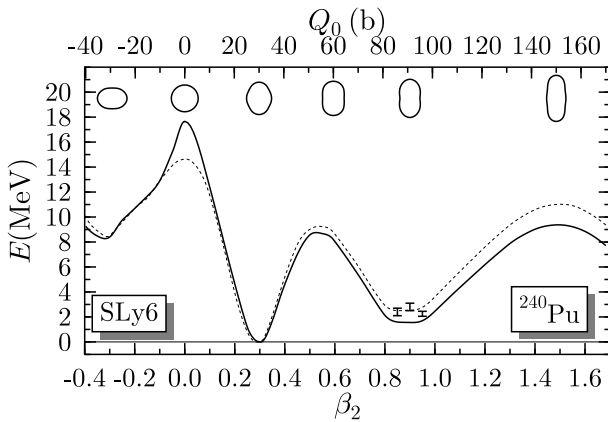


FIG. 2: Same as Figure 1, for the interaction SLy6.

and the relativistic mean-field method (RMF) [15]. Semi-classical approximations of the mean-field method were performed with different Skyrme forces in ref [16, 17]. Several Skyrme interactions and RMF Lagrangians were compared to the data in [18]. Axial and triaxial barriers obtained with Skyrme, Gogny and RMF forces are compared in Ref. [1]. Finally, the excitation energy of fission isomers has been studied with a variety of Skyrme forces in Ref. [5, 19].

The deformation energy curves obtained after particle-number projection and particle-number + angular-momentum projection on $J = 0$ are presented in Figures 1 and 2 for SLy4 and SLy6 interactions. For all curves, the energy of the ground state is taken as zero. The ground state and the fission isomer after projection are obtained from the mean-field minima. With the normalization that we have chosen to plot the results, the gain of energy obtained for the ground state by angular momentum projection is given by the difference between the curves at spherical shape. This gain is around 3.0 MeV for both interactions, bringing the calculated total energy closer to the experimental one.

The fission isomer is obtained at a β_2 value around 0.9; angular-momentum projection lowers its excitation energy by about 1 MeV for both forces, from 4.3 to 3.3 MeV for SLy4, and from 2.6 to 1.6 MeV for SLy6.

B. Rotational energy

Angular momentum projection provides the exact correction for the spurious rotational energy of the mean-field states. It is given by the difference between the binding energies before and after projection on angular momentum $J = 0$

$$E_{\text{rot}}(\beta_2) = E_{\text{mf}}(\beta_2) - E_{J=0}(\beta_2). \quad (4)$$

This difference does not depend much on the Skyrme parameterization and is plotted in the lower panel of Fig. 3 for SLy4. It is zero at spherical shape and increases first

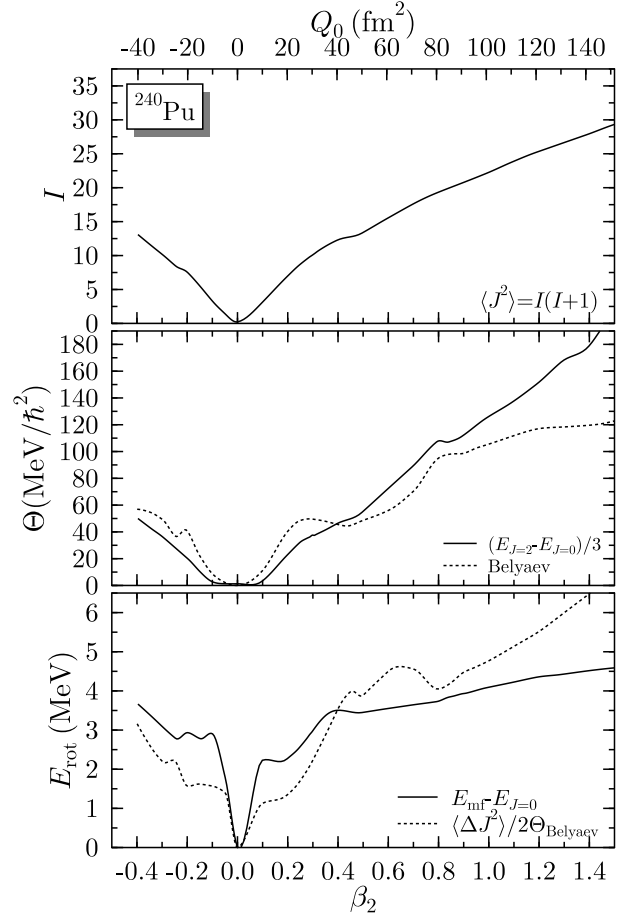


FIG. 3: Top to bottom: the average angular momentum I of the mean-field states obtained from $\langle J^2 \rangle = \hbar^2 I(I+1)$, the moment of inertia calculated from the difference of the projected $J = 2$ and $J = 0$ energy curves (solid line) and the Belyaev moment of inertia (dotted line); and the rotational energy obtained from the energy difference between the mean-field and the $J = 0$ energy curves (solid line) and the rotational correction, Eq. (5).

rapidly to values around 3 MeV for deformations smaller than $|\beta_2| < 0.1$, and then moderately for larger deformations. A similar behavior has been obtained in most of our previous calculations [4, 10]. The topology of the fission barrier is not much affected by angular momentum projection. The height of the second barrier is decreased by about 800 keV with respect to the fission isomer and by 1.5 MeV with respect to the ground state.

Rotational corrections are sometimes incorporated phenomenologically as a perturbation to mean-field calculations. In particular, it is an ingredient in the mass formulae based on Skyrme forces [20]. In the same way, the fission barrier of ^{240}Pu including a rotational correction was used as a constraint in the fit of the Gogny interaction [14]. In both cases, the rotational energy has the form

$$\tilde{E}_{\text{rot}}(\beta_2) = \frac{\langle J^2 \rangle_{\beta_2}}{2\Theta(\beta_2)}, \quad (5)$$

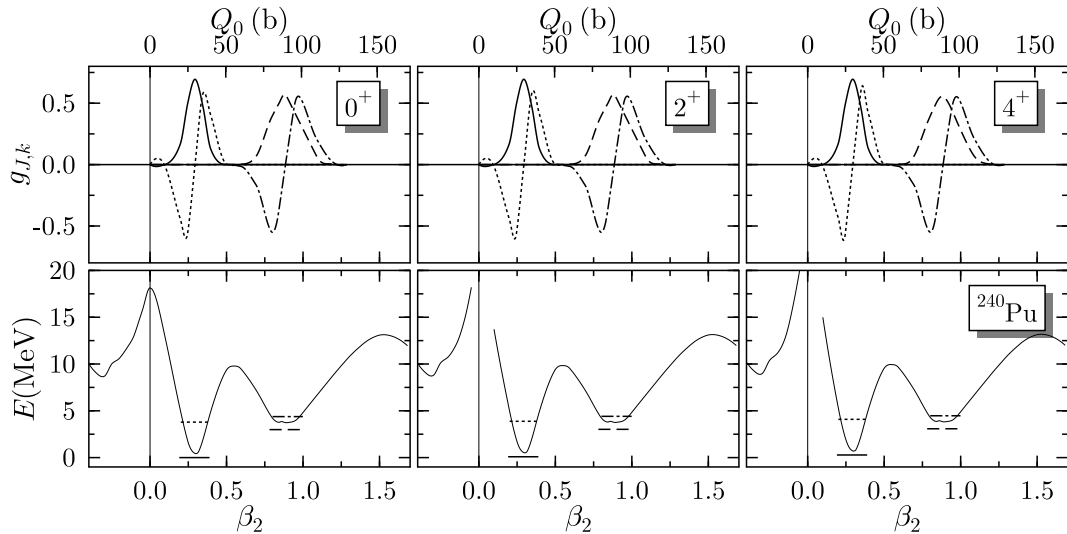


FIG. 4: Collective wave functions (upper panel) of the lowest 0^+ , 2^+ , and 4^+ states. The lower panels display the corresponding excitation energies at the average deformation of the mean-field states from which they are built, together with the projected energy curve.

where $\langle J^2 \rangle$ is the mean value of the square of the angular momentum for the mean-field state, and the moment of inertia Θ is determined from an approximate cranking formula

$$\Theta_{\text{Belyaev}} = 2 \sum_{i,j>0} \frac{|(i|\hat{J}_y|j)|^2}{E_i + E_j} (u_i v_j - v_i u_j). \quad (6)$$

The sum in Eq. (6) runs over the single-particle states $|i\rangle$ and $|j\rangle$ in a given deformed mean-field state, and E_i and E_j are the corresponding quasi-particle energies. For the large-scale mass fits of Ref. [20], the actual moment of inertia taken is a mixture of Eq. (6) and of the rigid-body moment of inertia. More involved approximations for the moment of inertia have been developed, see e.g. [21, 22] and references therein, but are rarely used. We can extract a moment of inertia from our projected mean-field calculations using the energy difference between the energy curves for $J = 0$ and $J = 2$ as

$$E_{J=I}(\beta_2) - E_{J=0}(\beta_2) = \frac{\hbar^2 I(I+1)}{2\Theta(\beta_2)}. \quad (7)$$

In Fig. 3, we compare the exact and approximate rotational energies as a function of deformation. We also show the angular momentum dispersion of the mean-field wave functions and the moment of inertia given by Eqn. (6) and obtained from the 2^+ excitation energy. Both of these moments of inertia are rather close for deformations around that of the fission isomer. For lower deformations, the Belyaev moment of inertia is significantly larger than the “exact” one. For larger deformations, the Belyaev moment does not increase as rapidly as the one extracted from our calculation. The dispersion of the angular momentum of the mean-field wave function increases also with deformation in a way which

is partly compensated by the increase of the Belyaev moment of inertia. However, this compensation is not strong enough and the Belyaev rotational energy correction overestimates at large deformations the energy correction obtained by exact projection. Note that this correction varies only by 1.5 MeV from the deformation corresponding to the ground state to the external fission barrier.

C. Configuration mixing

The properties of the four lowest states obtained from the configuration mixing calculation are given in Table I for SLy4 and Table II for SLy6. The corresponding collective wave functions are shown in Figure 4 for the SLy4 interaction. The states separate nicely into four rotational bands, two located in the prolate normal-deformed (ND) minimum, and two in the superdeformed (SD) one. The wave functions are all confined within either the ND or the SD wells. States obtained with SLy6 are similar, except for an overall shift in the excitation energies of the states located in the superdeformed well; the SD 0^+ band-head has an excitation energy of 2.99 MeV with SLy4 and 1.25 MeV with SLy6. The actual experimental value is in between the two, although there are some conflicting values given in the literature 2.4 ± 0.3 MeV [11], ≈ 2.8 MeV [23] and 2.25 ± 0.20 MeV [24].

The band head of the second ND band is obtained at 3.79 MeV for both forces. Similarly, the excitation energy of the second SD band with respect to the first SD band head is 1.39 MeV for SLy4 and 1.27 MeV for SLy6. This suggests that the excitation energies within a well are fairly independent from the surface tension of the Skyrme force. Both interactions give also similar values

state	E (MeV)	Q_s (e b)	$Q_0^{(s)}$ (e b)	$\beta_2^{(s)}$	$B(E2)\downarrow$ ($e^2 b^2$)	$Q_0^{(t)}$ (e b)	$\beta_2^{(t)}$
0_1^+	0.000	—	—	—	—	—	—
2_1^+	0.083	-3.4	11.9	0.300	2.80	11.9	0.300
4_1^+	0.277	-4.3	11.9	0.300	4.00	11.9	0.300
0_3^+	3.793	—	—	—	—	—	—
2_3^+	3.880	-3.4	11.9	0.301	2.82	11.9	0.301
4_3^+	4.088	-4.3	12.0	0.303	4.07	12.0	0.302
0_2^+	2.953	—	—	—	—	—	—
2_2^+	2.978	-10.3	36.0	0.911	25.8	36.0	0.911
4_2^+	3.045	-13.1	36.0	0.911	36.8	36.0	0.911
0_4^+	4.338	—	—	—	—	—	—
2_4^+	4.364	-10.4	36.5	0.922	26.4	36.5	0.922
4_4^+	4.429	-13.3	36.5	0.922	37.8	36.5	0.922

TABLE I: Properties of the rotational bands of ^{240}Pu obtained with SLy4: excitation energy E , spectroscopic quadrupole moment Q_s , corresponding quadrupole moment $Q_0^{(s)}$ and dimensionless deformation $\beta_2^{(s)}$ in the intrinsic frame, reduced $E2$ transition probability $B(E2)\downarrow$, and corresponding quadrupole moment $Q_0^{(t)}$ and dimensionless deformation $\beta_2^{(t)}$ in the intrinsic frame.

state	E (MeV)	Q_s (e b)	$Q_0^{(s)}$ (e b)	$\beta_2^{(s)}$	$B(E2)\downarrow$ ($e^2 b^2$)	$Q_0^{(t)}$ (e b)	$\beta_2^{(t)}$
0_1^+	0.000	—	—	—	—	—	—
2_1^+	0.083	-3.4	11.9	0.300	2.81	11.9	0.300
4_1^+	0.273	-4.3	11.9	0.301	4.02	11.9	0.301
0_4^+	3.794	—	—	—	—	—	—
2_4^+	3.879	-3.4	12.0	0.304	2.88	12.0	0.304
4_4^+	4.082	-4.4	12.1	0.306	4.15	12.1	0.305
0_2^+	1.251	—	—	—	—	—	—
2_2^+	1.277	-10.4	36.3	0.916	26.1	36.2	0.915
4_2^+	1.338	-13.2	36.3	0.917	37.4	36.3	0.916
0_3^+	2.519	—	—	—	—	—	—
2_3^+	2.550	-10.5	36.7	0.928	27.0	36.8	0.931
4_3^+	2.611	-13.4	36.7	0.928	38.3	36.7	0.928

TABLE II: The same as Table I, but for SLy6.

for the excitation energies within the bands.

The ground state band is known up to very high spin [25, 26, 27]. It has been suggested that static octupole deformation plays a role to explain the behaviour at large angular momentum Ref. [26, 28]. States below the 6^+ decay mainly by internal electron conversion, so the corresponding transitions have not been detected in γ -ray spectroscopy.

The lowest levels in the ground-state band are reported in the NUDAT data base [29] at 42.824 (2^+), 141.690 (4^+), and 294.319 keV (6^+). Our calculation overestimates these energies by almost a factor two. The experimental energies in the SD well are 20.1 keV for the 2^+

and 66.8 keV for the 4^+ for the SD1 band, and 769.9 (0^+), 785.1 (2^+), and 825.0 keV (4^+) for the SD2 band. They are also overestimated by our model. On the contrary, the calculated $B(E2; 2^+ \rightarrow 0^+)$ value is in excellent agreement with the experimental one of 26660 ± 360 $e^2 \text{ fm}^4$ obtained from Coulomb excitation [30].

A similar overestimation of excitation energies has been found for other nuclei with our model [2, 4] and in a similar framework using a Gogny interaction [31]. A hint on a possible origin of this discrepancy can be found from cranked mean-field calculations. In this case, neither configuration mixing nor restoration of symmetries are performed. However, time-reversal invariance is broken and the mean-field potential is optimised for each J value and not only for $J = 0$. An unprojected cranked HFB calculation [32] using the same effective interaction as here gives excitation energies for the ground-state band of 0.030 (2^+), 0.121 (4^+) and 0.271 MeV (6^+), respectively, in much better agreement with the data. Looking at Figure 4 one can see that, within a band, the amplitudes of the collective wave functions for different J values differ by less than 1% for each deformation. The wave functions for different J values are therefore probably too close to each other in our model. The slight breaking of time-reversal symmetry of mean-field states subject to a cranking constraint might be sufficient to provide a better starting point for exact projection and configuration mixing for the J different from 0 states.

The deformation of the ground state stays remarkably constant at all levels of approximations: from $\beta_2 = 0.29$ for the minima of the mean-field and projected energy curves to $\beta_2^{(s)}(2^+) = 0.30$ as deduced from Eqn. (3) for both the spectroscopic and the transition quadrupole moments. All these deformations agree with the one deduced from the experimental $B(E2)$ value, $\beta_2 = 0.29$.

Since we obtain nearly equal $\beta_2^{(s)}$ and $\beta_2^{(t)}$ values all along the bands, the use of the rotor model is well justified to describe the four bands.

We obtain also very large $E0$ transition matrix elements between states in the same well. With SLy4, the $M(E0; 0_3^+ \rightarrow 0_1^+)$ in the first well has a value of -29 $e \text{ fm}^2$ corresponding to $\rho(E0) = -0.52$, while the $M(E0; 0_4^+ \rightarrow 0_2^+)$ in the second well is 87 $e \text{ fm}^2$, or $\rho(E0) = 1.6$. As our model predicts the collective wave functions of all members of a rotational band to be very similar, the transition moments are calculated to be very similar as well for all $E0$ transitions within a band. The values obtained with the SLy6 interaction differ only marginally from those of SLy4. The $E0$ matrix elements that we obtain for transitions between states in the SD and the normal-deformed well are very small.

IV. DISCUSSION AND SUMMARY

The inclusion of correlations beyond mean-field confirms that many properties of the ^{240}Pu nucleus are already well described at the mean-field level of approxima-

tion. The overall structure of the potential energy curve is not altered by angular momentum projection, with a well defined prolate ground state and a fission isomer in narrow potential wells. Thanks to that, the properties of the lowest state in each well after configuration mixing are very close to the properties of the mean-field minima. The ground-state and fission isomer wave functions have a Gaussian shape and do not spread much around their respective minima. The superdeformed minimum in the potential energy surface is, however, too wide to confine completely the wave functions of the lowest SD band which are more spread, but still of Gaussian shape.

As expected, the total binding energy is slightly increased by angular momentum projection, and thereby comes closer to the experimental value. Compared to the ground state, angular-momentum projection lowers the (axial) inner barrier by about 0.6 MeV, the fission isomer by about 1 MeV, and the (reflection-symmetric) outer barrier by about 2 MeV. These changes of the potential landscape are going in the same direction as a decrease of the surface tension of the effective mean-field interaction and should therefore be considered when predicting superdeformed band heads and fission barrier heights. The schematic rotational correction used in the literature gives a too large reduction of the fission barrier heights by at least 2 MeV.

The energy of the superdeformed fission isomer turns out to be too low with SLy6, while for SLy4 it is slightly too high. We obtained similar results for SD band heads of Pb isotopes in the $A \approx 190$ region [5]. This suggests, that the surface tension might be too low for SLy6, while

it is slightly too high for SLy4. This is apparently in contradiction with Ref. [9], where it was argued on the basis of pure mean-field calculations for ^{240}Pu , that the surface tension of SLy6 is more realistic than that of SLy4. However, surface tension is not the only ingredient responsible for the energy of superdeformed states, as their existence is usually caused by a shell effect. Unfortunately, it is hard to disentangle the contribution from the macroscopic properties of the forces from the shell structure which is also not identical for SLy4 and SLy6 at large deformations.

The description of excited states in both wells is only partly satisfactory. While we obtain quite good results for $E2$ transition moments and deformations, neither the excitation energies of the excited 0^+ band heads nor the excitation energies within the bands are well reproduced. Unprojected cranked HFB calculations without any additional correlations perform much better for in-band transitions. This strongly suggests to extend our method to the use of such states as a starting set of wave functions. Such a development is currently underway. Using cranked mean-field states, however, will not change the too large excitation energies of 0^+ band heads.

Acknowledgments

This work was supported by the PAI-P5-07 of the PPS Scientific Policy. MB acknowledges support from the European Community. MB and PHH thank for the hospitality at the Institute for Nuclear Theory, Seattle, where this work was finalised.

[1] M. Bender, P.-H. Heenen, and P.-G. Reinhard, Rev. Mod. Phys. **75**, 121 (2003).

[2] A. Valor, P.-H. Heenen and P. Bonche, Nucl. Phys. **A671**, 145 (2000); M. Bender and P.-H. Heenen, Nucl. Phys. **A713** 390-401 (2003).

[3] T. Duguet, M. Bender, P. Bonche, P.-H. Heenen, Phys. Lett. **B559**, 201 (2003).

[4] M. Bender, P. Bonche, T. Duguet, P.-H. Heenen, Phys. Rev. C **69**, 064303 (2004).

[5] P.-H. Heenen, J. Dobaczewski, W. Nazarewicz, P. Bonche, and T. L. Khoo, Phys. Rev. C **57**, 1719 (1998).

[6] E. Chabanat, P. Bonche, P. Haensel, J. Meyer, and R. Schaeffer, Nucl. Phys. **A635**, 231 (1998), Nucl. Phys. **A643**, 441(E) (1998).

[7] C. Rigolet, P. Bonche, H. Flocard, P.-H. Heenen, Phys. Rev. C **59**, 3120 (1999).

[8] M. Samyn, S. Goriely, M. Pearson, private communication (2003).

[9] M. Bender, K. Rutz, P.-G. Reinhard, and J. A. Maruhn, Eur. Phys. J. **A7**, 467 (2000).

[10] M. Bender, H. Flocard and P.-H. Heenen, Phys. Rev. C **68**, 044321 (2003).

[11] S. Bjørnholm and J. E. Lynn, Rev. Mod. Phys. **52**, 725 (1980).

[12] H. J. Specht, Rev. Mod. Phys. **46**, 773 (1974); R. Van denbosch, Ann. Rev. Nucl. Part. Phys. **27**, 1 (1977); V. Metag, D. Habs, and H. J. Specht, Phys. Rep. **65**, 1 (1980); P. G. Thirolf and D. Habs, Prog. Part. Nucl. Phys. **49**, 325 (2002).

[13] H. Flocard, P. Quentin, D. Vautherin, M. Vénéroni, and A. K. Kerman, Nucl. Phys. **A231**, 176 (1974).

[14] M. Girod and B. Grammaticos Phys. Rev. C **27**, 2317 (1983); J.-F. Berger, M. Girod, and D. Gogny, Nucl. Phys. **A428**, 23c (1984); Nucl. Phys. **A502**, 85c (1989)

[15] V. Blum, J. A. Maruhn, P.-G. Reinhard, and W. Greiner, Phys. Lett. **B323**, 262 (1994); K. Rutz, J. A. Maruhn, P.-G. Reinhard, and W. Greiner, Nucl. Phys. **A590**, 680 (1995).

[16] A. K. Dutta and M. Kohno, Nucl. Phys. **A349**, 455 (1980); J. Bartel, P. Quentin, M. Brack, C. Guet, and H. -B. Häkansson, Nucl. Phys. **A** **386**, 79 (1982). M. Brack, C. Guet, and H.-B. Häkansson, Phys. Rep. **123**, 275 (1985);

[17] A. Mamdouh, J. M. Pearson, M. Rayet, and F. Tondeur, Nucl. Phys. **A644**, 389 (1998); Nucl. Phys. **A648**, 282(E) (1999); Nucl. Phys. **A679**, 337 (2001); A. K. Dutta, J. M. Pearson, and F. Tondeur, Phys. Rev. C **61**, 054303 (2000).

[18] T. Bürvénich, M. Bender, J. A. Maruhn, P.-G. Reinhard, Phys. Rev. C **69**, 014307 (2004).

- [19] S. Takahara, N. Tajima, and N. Onishi, Nucl. Phys. **A642**, 461 (1998).
- [20] S. Goriely, M. Samyn, M. Bender and J. M. Pearson, Phys. Rev. C **68**, 054325 (2003).
- [21] P. Ring and P. Schuck, *The Nuclear Many-Body Problem* (Springer, Berlin, 1980).
- [22] J. L. Egido, L. M. Robledo, in *Extended Density Functionals in Nuclear Physics*, G. A. Lalazissis, P. Ring, D. Vretenar [edts.], Lecture Notes in Physics **641** (Springer, Berlin and Heidelberg 2004), page 269.
- [23] B. Singh, R. Zywina, and R. B. Firestone, Nuclear Data Sheets **97**, 241 (2002).
- [24] M. Hunyadi, D. Gassmann, A. Krasznahorkay, D. Habs, P. G. Thirolf, M. Csatlós, Y. Eisermann, T. Faestermann, G. Graw, J. Gulyas, R. Hertenberger, H. J. Maier, Z. Mátáa, A. Metz, and M. J. Chromik, Phys. Lett. **B505**, 27 (2001).
- [25] G. Hackman, R. V. F. Janssens, T. L. Khoo, I. Ahmad, J. P. Greene, H. Amro, D. Ackermann, M. P. Carpenter, S. M. Fischer, T. Lauritsen, L. R. Morss, P. Reiter, D. Seweryniak, D. Cline, C. Y. Wu, E. F. Moore and T. Nakatsukasa, Phys. Rev. C **57**, R1056 (1998).
- [26] I. Wiedenhöver, R. V. F. Janssens, G. Hackman, I. Ahmad, J.P. Greene, H. Amro, P. K. Bhattacharyya, M. P. Carpenter, P. Chowdhury, J. Cizewski, D. Cline, T. L. Khoo, T. Lauritsen, C. J. Lister, A. O. Macchiavelli, D. T. Nisius, P. Reiter, E. H. Seabury, D. Seweryniak, S. Siem, A. Sonzogni, J. Uusitalo and C. Y. Wu, Phys. Rev. Lett. **83**, 2143 (1999).
- [27] R. V. F. Janssens, private communication, 2002.
- [28] R. K. Sheline, M. A. Riley, Phys. Rev. C **61**, 057301 (2000).
- [29] R. R. Kinsey *et al.*, *The NUDAT/PCNUDAT Program for Nuclear Data*, Data extracted from the NuDat2 database, version of 4/18/2004, at the National Nuclear Data Center WorldWideWeb site www.nndc.bnl.gov
- [30] C. E. Bemis, Jr., F. K. McGowan, J. L. C. Ford, Jr., W. T. Milner, P. H. Stelson, and R. L. Robinson, Phys. Rev. C **8**, 1466 (1973).
- [31] R. R. Rodriguez-Guzmán, J. L. Egido and L. M. Robledo, Phys. Rev. C **62**, 054308 (2000).
- [32] M. Bender, P. Bonche, T. Duguet, P.-H. Heenen, Nucl. Phys. **A723**, 35 (2003).